Behavior of a Power Conditioner for μ-SMES Systems Under Unbalanced Supply Voltages and Unbalanced Loads

D. Casadei, G. Grandi, U. Reggiani, G. Serra and A. Tani

University of Bologna, Department of Electrical Engineering
Viale Risorgimento 2, Bologna - 40136, Italy, elettro@mail.ing.unibo.it

Abstract - **In this paper a Power Conditioning System (PCS) is analyzed under input and output unbalanced conditions. The PCS, which can be utilized as active filter with additional tasks, consists of a voltage source inverter and a dc current chopper. The PCS considered in this paper uses a superconducting magnet as energy storage device. A theoretical analysis of the system behavior under unbalanced conditions is presented. Two control strategies are developed and compared with reference to the effects on the source power quality. Numerical simulations have been carried out by PSpice to verify the performance of the PCS in steady-state and transient operating conditions.**

I. Introduction

Recently, large attention has been paid on power quality improvement in industrial power systems by superconductivity technologies and power electronics, such as Micro Superconducting Magnetic Energy Storage (μ-SMES) [1]-[9]. The typical configuration of a μ-SMES based power conditioning system consists of a superconducting magnet and a set of power converters. The PCS can be series connected or shunt connected to the network. In general, the series connection is used for the compensation of voltage distortion in the supply network, and the protection of sensitive loads against voltage sags and swells. The shunt connection is used for the optimization of the source currents.

In this paper the attention is focused on a PCS connected in parallel with the network and the load. The system configuration is composed by a Voltage Source Inverter (VSI), a μ-SMES, and a current chopper for interfacing the superconducting magnet to the dc-link of the VSI (Fig. 1). Using this configuration it is possible to implement several control tasks such as reactive power compensation, active harmonic filtering, dynamic load balancing, and voltage flicker reduction. Furthermore, according to the stored magnetic energy, it is possible to compensate the line voltage for momentary outages. Some of this control tasks are typical also for standard active power filters [10]-[14]. This can be realized analyzing the PCS configuration given in Fig. 1, which includes a shunt active filter as a sub-system. The PCS represented in Fig. 1 has been analyzed in detail in [15]. It has been shown that, with an opportune controller design, several control tasks can be performed concurrently. This control capability can be utilized to meet a variety of applications, reducing the pay back time of the investment cost.

The study carried out in [15] is further developed in this paper to investigate the PCS performance under unbalanced supply voltages. It is known that, in a practical system, the supply is usually unbalanced to a certain extent and this may cause a distortion of source current if suitable control strategies are not employed.

The PCS control strategy described in [15] determines, at any instant, a source current vector with a constant magnitude, and in phase with the source voltage vector. In the case of unbalanced supply voltages, the negative sequence component causes variations in magnitude and angular speed of the source voltage vector. Under these operating conditions, the source currents become non-sinusoidal. In order to obtain sinusoidal source currents, two control strategies are proposed in this paper. The first one (*Strategy I*) is based on keeping the source current vector in phase with the positive sequence component of the supply voltages. This method leads to a current vector having constant magnitude and constant angular speed. The second one (*Strategy II*) is based on keeping the source current vector in phase with the source voltage vector, and with a magnitude proportional to that of the source voltage vector. This strategy leads to a source current vector similar to that of a pure resistive load.

The two control strategies have been analyzed using an approach similar to that proposed in [16] and [17].

Numerical simulations have been carried out to verify the behavior of the whole system in steady-state and transient operating conditions.

II. Description of the Control System

The behavior of the PCS is determined by three regulators, as represented in the block diagram shown in Fig. 2. The first regulator controls the energy stored in the superconducting magnet, the second one the dc-link voltage, and the third one the VSI ac currents. The analytical developments are carried out by representing the three-phase quantities with space vectors, according to a stationary *d-q* transformation [15].

In both control strategies, the reference value for the magnitude of the source current vector I_S^* is obtained by the regulator R_1. This regulator acts on the instantaneous error between the reference value of the energy stored in the Superconducting Coil (SC) E_{SC}^*, and its actual value E_{SC}, being $E_{SC} = \frac{1}{2} L_{SC} I_{SC}^2$.

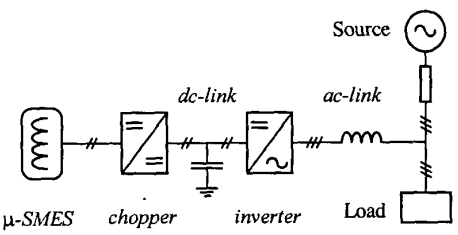

Fig. 1. Schematic drawing of the PCS structure.

The PWM current chopper performs the control of the dc-link voltage by means of the regulator R_2, keeping V_C close to its reference value V_C^*. In this way the energy stored in the capacitor is nearly constant and the active power flows directly from the Point of Common Coupling (PCC) to the SC, with exception of losses in converters and inductors.

The filter output currents are regulated by the VSI. The ac current control system requires the measurement of the load and filter currents $\bar{i}_L$ and $\bar{i}_F$. The load current is used to calculate the reference value of the filter current $\bar{i}_F^*$, on the basis of the reference source current $\bar{i}_S^*$, given by the SC energy regulator, as follows $\bar{i}_F^* = \bar{i}_S^* - \bar{i}_L$. The value obtained for $\bar{i}_F^*$ is the VSI input command and can be utilized to implement either hysteresis or PWM current regulators. A hysteresis current regulator acting on the instantaneous current error $\Delta\bar{i}_F = \bar{i}_F^* - \bar{i}_F$ can be employed to determine the inverter switch states S_A, S_B, S_C. Alternatively, a PWM current regulator can be used avoiding the drawbacks of hysteresis current controllers. In this case, the reference voltage for the inverter can be calculated by the voltage equation written across the link inductance L. Neglecting the resistive effects, and introducing a variational model, this equation yields

$$\bar{v}_F^* = \bar{v}_S - \frac{L}{\Delta t}\Delta\bar{i}_F .$$

III. PCS Basic Equations

The instantaneous output power of the PCS equals the difference between the instantaneous power required by the load and the instantaneous power delivered by the source.

The instantaneous output power of the PCS can be expressed by the following scalar product

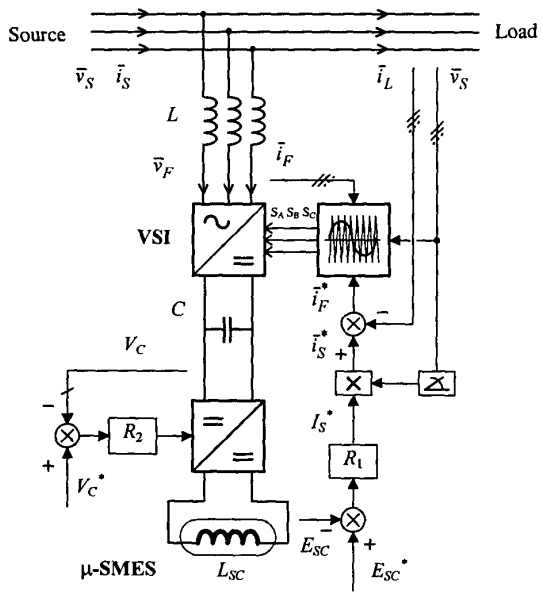

Fig. 2. Block diagram of the PCS control scheme.

$$p_F = \tfrac{3}{2}\bar{v}_S \cdot \bar{i}_F \tag{1}$$

In (1) and in the following equations, the subscript $_F$ denotes PCS quantities.

In order to show the effects of the PCS on source currents, (1) can be rewritten as

$$p_F = \tfrac{3}{2}\bar{v}_S \cdot \left(\bar{i}_S - \bar{i}_L\right) \tag{2}$$

In (2) the source voltage and the load current are given quantities whereas the source current depends on the PCS mode of operation.

In steady-state conditions, the instantaneous output power of the PCS can be represented by the sum of a dc component p_{F0} and an alternating component $\tilde{p}_F$, according to

$$p_F = p_{F_0} + \tilde{p}_F \tag{3}$$

In steady-state conditions the average value of the power delivered by the PCS is zero, and the average value of the source power equals the average value of the load power.

Then, the basic equation describing the steady-state power flow through the PCS is

$$p_{F_0} = 0 \tag{4}$$

In the next Section, Eq. (4) is further developed for different operating conditions.

IV. PCS Operation Under Balanced Voltages

When the source voltages are balanced, the corresponding space vector can be expressed as

$$\bar{v}_S = \bar{V}_{S_1} e^{j\omega t} \tag{5}$$

In (5) and in the following equations the capital letters represent constant quantities.

In general, non-linear and unbalanced loads determine unbalanced non-sinusoidal load currents, which can be expanded in complex Fourier series as follows

$$\bar{i}_L = \sum_{k=-\infty}^{\infty} \bar{I}_{L_k} e^{jk\omega t} \tag{6}$$

In the same way the source current vector can be expressed as

$$\bar{i}_S = \sum_{k=-\infty}^{\infty} \bar{I}_{S_k} e^{jk\omega t} \tag{7}$$

Substituting (5), (6) and (7) into (2) leads to

$$p_F = \frac{3}{2}\bar{V}_{S_1} e^{j\omega t} \cdot \left[\sum_{k=-\infty}^{\infty}\left(\bar{I}_{S_k} - \bar{I}_{L_k}\right) e^{jk\omega t}\right] \tag{8}$$

By developing (8) it is possible to determine p_{F0}, and substituting its expression in (4) yields

$$p_{F_0} = \frac{3}{2}\bar{V}_{S_1} \cdot \left(\bar{I}_{S_1} - \bar{I}_{L_1}\right) = 0 \tag{9}$$

This simple equation represents a constraint for the source current fundamental component and must be taken into account when defining the reference value of the source current in the SC energy control loop.

V. PCS Control Strategy Under Balanced Voltages

The basic principle of the control system is to impose sinusoidal source currents, in phase with the corresponding line-to-neutral source voltages. According to this principle, the source current vector can be expressed as

$$\bar{i}_S = \frac{\bar{V}_{S_1}}{A} e^{j\omega t} = \bar{I}_{S_1} e^{j\omega t} \tag{10}$$

where the constant A must be defined to satisfy Eq. (9).

In this way the source currents are balanced and sinusoidal, as in the case of a pure resistive load.

Substituting (10) in (9) and solving for A yields

$$A = \frac{\left|\bar{V}_{S_1}\right|^2}{\bar{V}_{S_1} \cdot \bar{I}_{L_1}} \tag{11}$$

This equation could be utilized to calculate the value of A, once the source voltage and the fundamental component of the load current are known. In the control scheme represented in Fig. 2, the opportune value of A is determined through the action of the regulator R_1.

VI. PCS Operation Under Unbalanced Voltages

When the source voltages are unbalanced, the corresponding space vector can be expressed in terms of positive and negative sequence components as

$$\bar{v}_S = \bar{V}_{S_1} e^{j\omega t} + \bar{V}_{S_{-1}} e^{-j\omega t} \tag{12}$$

Substituting (12), (6) and (7) into (2) leads to

$$p_F = \frac{3}{2}\left[\bar{V}_{S_1} e^{j\omega t} + \bar{V}_{S_{-1}} e^{-j\omega t}\right] \cdot \left[\sum_{k=-\infty}^{\infty} \left(\bar{I}_{S_k} - \bar{I}_{L_k}\right) e^{jk\omega t}\right] \tag{13}$$

By developing (13), it is possible to determine p_{F0}, and Eq. (4) becomes

$$p_{F_0} = \frac{3}{2}\left[\bar{V}_{S_1} \cdot \left(\bar{I}_{S_1} - \bar{I}_{L_1}\right) + \bar{V}_{S_{-1}} \cdot \left(\bar{I}_{S_{-1}} - \bar{I}_{L_{-1}}\right)\right] = 0 \tag{14}$$

This equation is equivalent to (9) in the case of unbalanced supply voltages. Here the constraint is applied to both the positive and negative sequence fundamental components of the source current.

In these operating conditions, the determination of a control strategy is not so immediate as in the case of balanced supply voltages. In the next Section, two possible control strategies are presented and discussed.

VII. PCS Control Strategies Under Unbalanced Voltages

A. Strategy I

The basic principle is to impose sinusoidal source currents, characterized by a space vector having constant magnitude and in phase with the positive sequence fundamental component of the source voltage. This control strategy can be represented by the following equation

$$\bar{i}_S = \frac{\bar{V}_{S_1} e^{j\omega t}}{A'} \tag{15}$$

Substituting (15) in (14) and solving for A' yields

$$A' = \frac{\left|\bar{V}_{S_1}\right|^2}{\bar{V}_{S_1} \cdot \bar{I}_{L_1} + \bar{V}_{S_{-1}} \cdot \bar{I}_{L_{-1}}} \tag{16}$$

The value of A' could be calculated by (16), but this equation would require a large computational time for the implementation. In the control scheme of Fig. 2, the value of A', and then the magnitude of the source current vector, is set directly by the regulator R_1. The implementation of *Strategy I* requires the estimated value $\hat{\bar{V}}_{S_1}$ of the positive sequence fundamental component of the source voltage vector, according to (15). For this purpose, it can be noted that the negative sequence fundamental component and the harmonic components of the source voltages have zero dc value in a synchronous reference frame. Then, by applying an opportune low-pass filter to the source voltage vector in a synchronous reference frame, it is possible to extract the value of $\hat{\bar{V}}_{S_1}$. In this paper, in order to improve the estimation of $\hat{\bar{V}}_{S_1}$, a second order low-pass filter has been used. The behavior of the low-pass filter can be expressed in terms of d and q variables by the following equations

$$\Re e\left(\hat{\bar{V}}_{S_1}^s\right) \cong \Re e\left(\hat{\bar{v}}_{S_1}^s\right) = \frac{1}{(1+\tau s)^2} \Re e\left(\bar{v}_S^s\right) \tag{17}$$

$$\Im m\left(\hat{\bar{V}}_{S_1}^s\right) \cong \Im m\left(\hat{\bar{v}}_{S_1}^s\right) = \frac{1}{(1+\tau s)^2} \Im m\left(\bar{v}_S^s\right) \tag{18}$$

In (17) and (18) the superscript ^{s} denotes quantities in the synchronous reference frame. Eqs. (17) and (18) can be rewritten in the stationary reference frame leading to

$$\hat{\bar{V}}_{S_1} e^{j\omega t} \cong \hat{\bar{v}}_{S_1} = \frac{1}{\left(1+\tau s - j\omega\tau\right)^2} \bar{v}_S \tag{19}$$

By measuring the instantaneous values of the source voltages and applying the d-q transformation, it is possible to calculate $\bar{v}_S$. Then, by using (19) the value of $\hat{\bar{V}}_{S_1} e^{j\omega t}$ can be readily estimated and utilized to modulate the output of R_1.

B. Strategy II

The basic principle is to impose a source current vector in phase with the source voltage vector, and with a magnitude proportional to that of the voltage vector itself. This means that the load is conditioned to behave as a pure resistive load. The control strategy so defined can be represented by the following equation

$$\bar{i}_S = \frac{\bar{v}_S}{R_{eq}} = \frac{\bar{V}_{S_1} e^{j\omega t} + \bar{V}_{S_{-1}} e^{-j\omega t}}{R_{eq}} \tag{20}$$

Substituting (20) in (14) and solving for R_{eq} yields

$$R_{eq} = \frac{\left|\bar{V}_{S_1}\right|^2 + \left|\bar{V}_{S_{-1}}\right|^2}{\bar{V}_{S_1} \cdot \bar{I}_{L_1} + \bar{V}_{S_{-1}} \cdot \bar{I}_{L_{-1}}} \tag{21}$$

This equation is equivalent to (16) of *Strategy I*. In this case also it is possible to use the regulator R_l to determine the reference value for the source current. The difference between *Strategy I* and *Strategy II* is that in the first case the output of R_l is modulated by $\bar{v}_{S_1} = \bar{V}_{S_1} e^{j\omega t}$, whereas in the second case the output of R_l is modulated by $\bar{v}_S$.

C. Comparison between Strategy I and Strategy II

With reference to the possibility to implement the two control strategies on a DSP based controller, it can be noted that *Strategy II* is more simple because it does not require the calculation of the source voltage positive sequence through the low-pass filter.

In the case of balanced source voltages the two control strategies behave in the same way, determining for a given load the same source currents.

In the case of unbalanced source voltages, according to (15) and (20), the two control strategies determine source currents which are balanced sinusoidal using *Strategy I*, and unbalanced sinusoidal using *Strategy II*. It can be noted that, in some cases, unbalanced source currents could be preferred to balanced source currents. As an example, let us to consider the unbalance introduced by an overload condition of one network phase, causing a decrease of the corresponding line-to-neutral source voltage. In this case, *Strategy II* imposes sinusoidal currents with a lower amplitude in the overloaded phase.

A further comparison can be developed with reference to the instantaneous value of the source power, that can be expressed as

$$p_S = \frac{3}{2}\bar{v}_S \cdot \bar{i}_S \tag{22}$$

In the case of *Strategy I*, substituting (12) and (15) in (22), leads to

$$p_S^I = \frac{3}{2A'}\left[\left|\bar{V}_{S_1}\right|^2 + \Re_e\left(\bar{V}_{S_1}\bar{V}_{S_{-1}}^* e^{j2\omega t}\right)\right] \tag{23}$$

Taking (16) into account, (23) becomes

$$p_S^I = \frac{3}{2}\left(\bar{V}_{S_1}\cdot\bar{I}_{L_1} + \bar{V}_{S_{-1}}\cdot\bar{I}_{L_{-1}}\right)\left[1 + \Re_e\left(\frac{\bar{V}_{S_{-1}}}{\bar{V}_{S_1}} e^{-j2\omega t}\right)\right] \tag{24}$$

As it could be expected, the instantaneous source power is composed of two terms. The first one is constant and the second one is pulsating with angular frequency 2ω.

In the case of *Strategy II*, substituting (12) and (20) in (22) leads to

$$p_S^{II} = \frac{3}{2R_{eq}}\left[\left|\bar{V}_{S_1}\right|^2 + \left|\bar{V}_{S_{-1}}\right|^2 + 2\Re_e\left(\bar{V}_{S_1}\bar{V}_{S_{-1}}^* e^{j2\omega t}\right)\right] \tag{25}$$

Taking (21) into account, (25) becomes

$$p_S^{II} = \frac{3}{2}\left(\bar{V}_{S_1}\cdot\bar{I}_{L_1} + \bar{V}_{S_{-1}}\cdot\bar{I}_{L_{-1}}\right)\left[1 + 2\Re_e\left(\frac{\bar{V}_{S_1}\bar{V}_{S_{-1}}^*}{\left|\bar{V}_{S_1}\right|^2 + \left|\bar{V}_{S_{-1}}\right|^2} e^{j2\omega t}\right)\right] \tag{26}$$

By comparing (24) to (26), it appears that under unbalanced source voltages the constant term of the source power is the same for both strategies, whereas the pulsating term is greater using *Strategy II*.

VIII. Simulation Results

In order to verify the performance of the PCS, two different circuit models have been implemented using PSpice.

The first model considers both the inverter and the chopper as ideal converters, that is the switching effects are neglected. Under this assumption the electrical quantities are represented by their averaged values. This simplified model requires very low computational times (few tens of seconds) and it has been employed to tune the regulators parameter.

The second model is implemented considering the power IGBT as ideal switches, that is with instantaneous lossless commutations. In this case the electrical quantities obtained by the numerical simulations are expected to be very close to the corresponding real quantities because of the presence of the switching effects.

The numerical simulations have been carried out with reference to a 380V, 50Hz three-phase supply system. The source impedance has been represented by series *R-L* parameters.

A. Steady-state performance

By means of the second model, four significant cases have been investigated emphasizing the system behavior in different operating conditions. The corresponding numerical results have been represented in terms of vector loci in the *d-q* plane and are shown from Fig. 3 to Fig. 6. The vectors shown in these figures represent the electrical quantities at the same time instant. In this way, the phase angle relationships are emphasized.

B. Case 1

In this case the operating conditions are characterized by balanced supply voltages and unbalanced load (20% negative sequence). Fig. 3 shows the loci of the source voltage $\bar{v}_S$, source current $\bar{i}_S$, load current $\bar{i}_L$, and filter current $\bar{i}_F$, obtained using either *Strategy I* or *Strategy II*.

The PCS delivers the fundamental reactive component of the load current, as well as the negative sequence component. Being the supply voltage balanced, the negative sequence component of the load current is fully supplied by the PCS. Then, the loci of the source voltage and current are circular whereas the loci of the filter current and load current are elliptical.

C. Case 2

In the second case the operating conditions are characterized by balanced supply voltages and non-linear load (3-phase diode rectifier). Fig. 4 shows the voltage and current loci obtained using either *Strategy I* or *Strategi II*.

Owing to the active filtering capability of the PCS, the source current vector locus is close to a circle. This means that the source currents are almost sinusoidal despite of the non-linearities of the load.

D. Case 3

In the third case the operating conditions are characterized by an unbalanced supply voltages (20% negative sequence) and balanced load. Fig. 5 shows the voltage and current loci obtained using the *Strategy II.*

In this case the source line currents are proportional to the corresponding source line-to-neutral voltages. Then, the source voltage and current vectors describe two similar ellipses. This means that the unbalance degree of the source voltages is directly reflected on the source currents.

E. Case 4

In this case the operating conditions are the same as in Case 3, but *Strategy I* is used instead of *Strategy II.* Fig. 6 shows the voltage and current loci obtained by numerical simulations.

Owing to the features of *Strategy I*, the resulting source currents are balanced and sinusoidal. The PCS behaves as an active filter compensating at the same time the negative sequence current component and the reactive power of the load. The source current vector is in phase with the source voltage positive sequence component, and oscillates around the source voltage vector.

F. Transient performance

The dynamic behavior of the PCS has been tested during the switching-on and switching-off of the load. The operating conditions are characterized by balanced supply voltages and unbalanced load as in Case 1. Fig. 7 shows the simulation results obtained. *Strategies I* and Strategy *II* lead to the same results, being the supply voltages balanced.

Figs. 7a and 7b show the source currents i_{Sa}, i_{Sb} and i_{Sc} and the load currents i_{La}, i_{Lb} and i_{Lc},. Due to the presence of the PCS, the source currents are balanced showing smooth amplitude variations in response to step variation of the load currents. This behavior is particularly significant for the reduction of flicker effects.

Fig. 7c shows the dc-link voltage V_C. The regulator R_2 ensures small voltage variations, even with 100% load changes. The 100 Hz voltage oscillation is related to the pulsating instantaneous power required to balance the load currents.

Fig. 7d represents the behavior of the superconducting coil current I_{SC}. The SC delivers energy during the load switching-on transient. This energy is recovered by the SC during the load switching-off transient, allowing the SC current to restore its rated value. The small oscillations of the SC current are introduced by the PCS operation for compensating the instantaneous pulsating power demanded by the unbalanced load. In this energy exchange process the capacitor is not involved being the dc-link voltage practically constant.

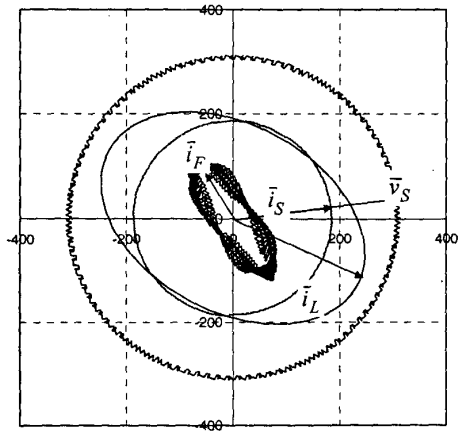

Fig. 3 - Voltage and current loci related to Case 1.

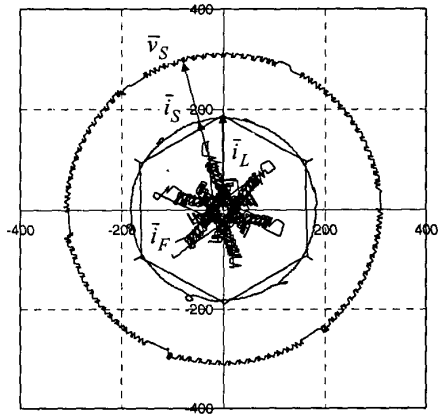

Fig. 4 - Voltage and current loci related to Case 2.

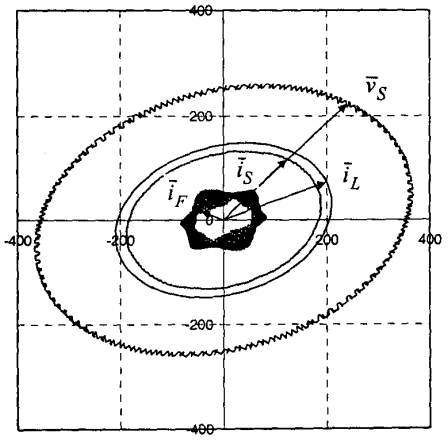

Fig. 5 - Voltage and current loci related to Case 3.

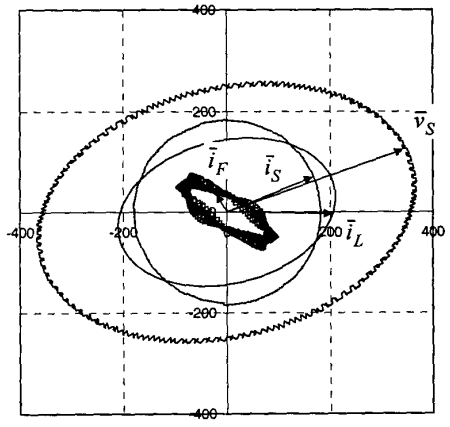

Fig. 6 - Voltage and current loci related to Case 4.

Figs. 7e, 7f, and 7g show the instantaneous power absorbed by the load p_L, supplied by the source p_S, and absorbed by the filter p_F, respectively. The 100 Hz fluctuations of p_L (Fig. 7e) are due to the load unbalance. These oscillations are compensated by the PCS, leading to the smooth instantaneous source power p_S shown in Fig. 7f. The compensating instantaneous power absorbed by the PCS is shown in Fig. 7g.

IX. CONCLUSIONS

A control scheme for power conditioning systems, in which a μ-SMES is employed for energy storage, has been analyzed in this paper.

The main feature of the proposed power conditioning system is the possibility to solve simultaneously several power quality problems. This feature cannot be completely achieved in presence of unbalanced supply voltages if suitable control strategies are not employed.

In this paper, two control strategies which allow good performance to be obtained, even with unbalanced supply voltages, have been presented and discussed. The first one determines sinusoidal and balanced source currents. The second one determines sinusoidal source currents with the same unbalance of the source voltages.

These strategies have been compared emphasizing advantages and disadvantages in different operating conditions.

Several numerical simulations have been carried out for the two control strategies, showing their capability for power quality improvement when non-linear and pulsating loads are connected to the network.

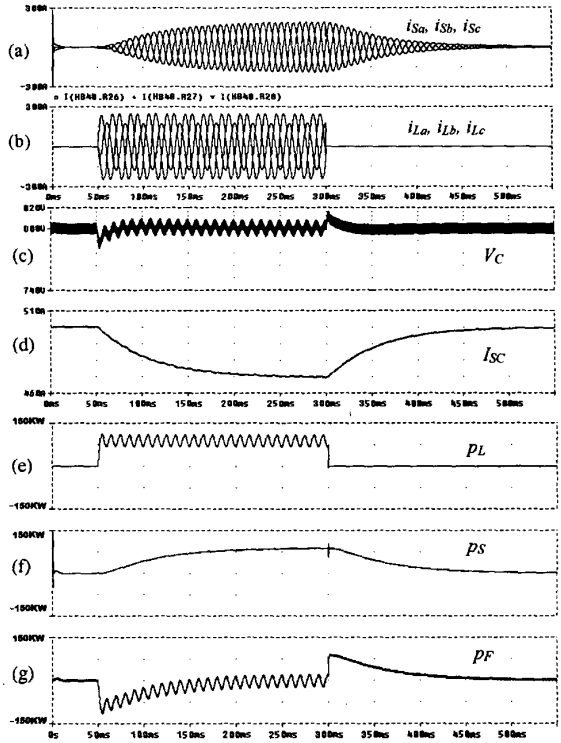

Fig. 7 - Transient performance of the PCS during the switching-on and the switching-off of the load.

REFERENCES

[1] H.J. Boeing, J.F. Hauer, "Commissioning Test of the Bonneville Power Administration 30 MJ Superconducting Magnetic Energy Storage Unit," IEEE Trans. on PAS, Vol. 104, pp. 302-312, February 1985.

[2] R.L. Kustom, J.J. Skiles, J. Wang, "Power Conversion System for Diurnal Load Levelling with Superconducting Magnetic Energy Storage," IEEE trans. on Magnetics, Vol. 23, September 1987.

[3] R.L. Lasseter, S.G. Jalai, "Dynamic Response of Power Conditioning Systems for Superconductive Magnetic Energy Storage," IEEE Trans. Energy Conversion, Vol. 6, pp. 388-393, September 1991.

[4] R.L. Kustom, J.J. Skiles, J. Wang, K. Klontz, T. Ise, K. Ko, F. Vong, "Research on Power Conditioning Systems for Superconductive Magnetic Energy Storage (SMES)," IEEE Trans. on Magnetics, Vol. 27, pp. 2320-2323, March 1991.

[5] I. D. Hassan, R.M. Bucci, K.T. Swe, "400MW SMES Power Conditioning System Development and Simulation," IEEE Trans. Power Electronics, Vol. 8, pp. 237-249, July 1993.

[6] M. Tada, Y. Mitani, K. Tsuji, " Power Control by Superconducting Magnetic Energy Storage for Load Change Compensation and Power System Stabilization in Interconnected Power System," IEEE Trans. on Applied Superconductivity, Vol. 5, pp. 250-253, June 1995.

[7] J.J. Skiles, R.L. Kustom, K. Ko, "Performance of a Power Conversion System for Superconducting Magnetic Energy Storage (SMES)," IEEE Trans. on Power Systems, Vol. 11, pp. 1718-1723, November 1996.

[8] I.J. Iglesias, J. Acero, A. Bautista, "Comparative Study and Simulation of Optimal Converter Topologies for SMES Systems," IEEE Trans. on Applied Superconductivity, Vol. 5, pp. 254-257, June 1995.

[9] I. J. Iglesias, A. Bautista, M. Visiers, "Experimental and Simulated Results of a SMES Fed by a Current Source Inverter," IEEE Trans. on Applied Superconductivity, Vol. 7, pp.861-864, June 1997.

[10] L.Gyugyi, E.C.Strycula, "Active AC Power Filter," Proc. IEEE-IAS Annual Meeting, pp. 529, 1976.

[11] H.Akagi, Y.Kanazawa, A.Nabae, "Instantaneous Reactive Power Compensators Comprising Switching Devices without Energy Storage Components," IEEE Trans. on IA, Vol. 20, pp. 625, 1984.

[12] L.Malesani, L.Rossetto, P.Tenti, "Active Filters for Reactive Power and Harmonic Compensation," Proc. IEEE-PESC, pp. 321-330, June 1986.

[13] O. Simon, H. Spaeth, K.P. Juengst, P. Komarek, "Experimental Setup of a Shunt Active Filter Using a Superconducting Magnetic Energy Storage Device," Proc. EPE'97, Vol.1, pp. 447-452, September 1997.

[14] D. Casadei, G. Grandi, U. Reggiani, C. Rossi, "Control Methods for Active Power Filters with Minimum Measurement Requirements," Proc. APEC'99 Conference, Dallas TX (USA), March 14-18, 1999.

[15] D. Casadei, G. Grandi, U. Reggiani, G. Serra, "Analysis of a Power Conditioning System for Superconducting Magnetic Energy Storage (SMES)," Proc. IEEE-ISIE'98, Pretoria (South Africa), July 7-10, 1998, Vol. 2, pp. 546-551.

[16] D. Casadei, G. Serra, A. Tani, "Reduction of the input current harmonic content in matrix converter under input/output unbalance," *IEEE Trans. on Ind. Elec.*, Vol. 45 No. 3, June 1998, pp. 401-411.

[17] D. Casadei, G. Serra, A. Tani. "A general approach for the analysis of the input power quality in matrix converter," *IEEE Trans. on Power Electronics*, Vol. 13, No. 5, September 1998, pp. 882-891.